Nucl. Sci. and Tech., Vol.9, No. 4 (2019), pp. 27-33

Nuclear Science and Technology

Journal homepage: https://jnst.vn/index.php/nst

Determination of in situ detection efficiency for IM-NAA of non-standard geometrical samples

Nguyen Duy Quang[1], Trinh Van Cuong[1], Tran Tuan Anh[1], Ho Van Doanh[1], Nguyen Thi Tho[1], Ho Manh Dung[2]

[1] *Dalat Nuclear Research Institute, 01 Nguyen Tu Luc Street., Da Lat, Lam Dong*

[2] *Center For Nuclear Techniques, 217 Nguyen Trai street, District 1, HCM City*

Email: duyquang1691@gmail.com

Abstract: The k0-based internal mono-standard (IM) method was first proposed for the concentration analysis of samples of non-standard geometry in the 2000s. The method has demonstrated several advantages such as the elimination of gamma-ray self-attenuation and geometrical effects. On the other hand, the accuracy of the method principally depends on the in situ relative detection efficiency, which requires to be obtained in each measurement. Therefore, the relative detection efficiency is always under consideration for the improvement of the analysis results. The present paper describes a simple and automatic procedure for the determination of the relative efficiency using one or more activation products emitting gamma rays over a considered range of the spectrum. The procedure can be applied for INAA and PGNAA analysis.

Keywords: *INAA, PGNAA, internal mono-standard method, relative efficiency, non-standard geometry samples.*

I. INTRODUCTION

Neutron activation analysis (NAA) is a sensitive multi-element analytical technique used for both qualitative and quantitative analysis of elements in a vast amount of materials. The technique has applications in chemistry, geology, archeology, medicine, environmental monitoring and even in forensic science [1-4]. However, there are limitations due to sample size for application in bulk analysis, in particular for archaeology and cultural art artifacts, forensic materials as well as geological studies . For example, large and non-standard geometry samples give rise to problems of neutron self-shielding, gamma rays attenuation and certain geometrical effects. Therefore, the internal mono-standard analysis method has been proposed to overcome the mentioned difficulties [5]. In this method, the in situ relative detection efficiency is required to be obtained in each measurement and then used for elemental concentration analysis. The in situ relative detection efficiency plays a key role in the analysis as it is valuable to the correction of sample geometry effects [6]. In this study, a computer code for the determination of the in situ relative efficiency has been developed. Using Prompt Gamma NAA (PGNAA) and Instrumental NAA (INAA) nuclear data, the software requires only a peak area report file for calculation of relative efficiency and perform further analysis. Results from measurements of standard reference materials have been found to be in good agreement with certified values.

https://doi.org/10.53747/jnst.v9i4.138
Received 29 November 2019, accepted 30 December 2019
©2019 Vietnam Atomic Energy Society and Vietnam Atomic Energy Institute

II. CONTENT

A. Subjects and methods

In INAA using k_0 approach, consider two arbitrary elements x and y presented in an activated sample which emits two series of characteristic gamma rays $E_{x,i}$ and $E_{y,j}$ (i, j = 1, 2,...), respectively. The mass ratio of element x to y can be expressed as follow [5]:

$$\frac{m_x}{m_y} = \frac{(SDC(f+Q_0(\alpha)))_y}{(SDC(f+Q_0(\alpha)))_x} \frac{P_{E_{x,i}}\varepsilon_{E_{y,j}}}{P_{E_{y,j}}\varepsilon_{E_{x,i}}} \frac{k_{0,E_{y,j}}}{k_{0,E_{x,i}}} \quad (1)$$

Where S is the saturation factor, D is the decay factor, C is the measurement factor, f is the ratio of the thermal to epithermal neutron fluxes, $Q_0(\alpha)$ is the ratio of the resonance integral-to-thermal neutron cross-section corrected for the non-ideal epithermal neutron flux distribution (α), P is the peak area and ε is the full energy peak detection efficiency. In case of high f, the value of $(f+Q_0(\alpha)))_y / (f+Q_0(\alpha)))_x$ in eq. (1) tends to unity and therefore, eq. (1) can be simplified as:

$$\frac{m_x}{m_y} = \frac{(SDC)_y}{(SDC)_x} \frac{P_{E_{x,i}}\varepsilon_{E_{y,j}}}{P_{E_{y,j}}\varepsilon_{E_{x,i}}} \frac{k_{0,E_{y,j}}}{k_{0,E_{x,i}}} \quad (2)$$

The situation is very simple in case of PGNAA where the correction factors S, D and C can be eliminated. Though, it should be noted that the k_0 databases for two different techniques are different. Having it in mind, the mass ratio in both INAA and PGNAA can be rewritten as:

$$\frac{m_x}{m_y} = \frac{c_{E_{x,i}}}{c_{E_{y,j}}} \frac{\varepsilon_{E_{y,j}}}{\varepsilon_{E_{x,i}}} \quad (3)$$

Where c is the coefficient calculated using k_0 database and experimental data

$$c_{E_{x,i}} = \frac{P_{E_{x,i}}}{(SDC)_x \times (f+Q_0(\alpha)))_x \times k_{0,E_{x,i}}} \quad (4)$$

and in some cases can be simplified as

$$c_{E_{x,i}} = \frac{P_{E_{x,i}}}{(SDC)_x \times k_{0,E_{x,i}}} \quad (5)$$

As clearly seen in eq. (3), the relative concentration of element x to y can be determined by the ratio of full peak detection efficiencies. This leads to the need for using relative detection efficiency which can be determined straightforwardly from eq. 3 using a fitting procedure. The relation of detection efficiencies is as follow:

$$\varepsilon_{E_{y,j}} = \frac{c_{E_{x,i}}}{c_{E_{y,j}}} \frac{m_x}{m_y} \varepsilon_{E_{x,i}} \quad (6)$$

Hence,

$$\ln(\varepsilon_{E_{y,j}}) = \ln\left(\frac{m_x}{m_y}\right) + \ln\left(\frac{c_{E_{x,i}}}{c_{E_{y,j}}}\right) + \ln(\varepsilon_{E_{x,i}}) \quad (7)$$

The efficiencies at different gamma energies of each element are derived from eq. (6)

$$\ln(\varepsilon_{E_{x,i}}) = \ln\left(\frac{c_{E_{x,1}}}{c_{E_{x,i}}}\right) + \ln(\varepsilon_{E_{x,1}}), i = 2,3,... \quad (8)$$

$$\ln(\varepsilon_{E_{y,j}}) = \ln\left(\frac{c_{E_{y,1}}}{c_{E_{y,j}}}\right) + \ln(\varepsilon_{E_{y,1}}), j = 2,3,... \quad (9)$$

Thus, relative efficiency curves in logarithmic scale constructed individually from each element are expected to be differed by constant factors, say t. Because of using relative efficiency, an arbitrary positive value can be firstly assigned to one detection efficiency of each element, e.g. $\mathrm{Arb}\,\varepsilon_{E_{k,1}} = 10\%$ for any k-th element where "Arb" indicates the first choice of detection efficiency. The relative detection efficiencies are then corrected by t-factors:

$$\ln(\mathrm{Rel}\varepsilon_{E_{k,i}}) = \ln(\mathrm{Arb}\varepsilon_{E_{k,i}}) + t_k \qquad (10)$$

In general, the expression for the relative efficiency curve is

$$\ln(\mathrm{Rel}\varepsilon(E)) = \sum_{i=0}^{n} a_i (\ln E)^i \qquad (11)$$

Where a_i is the coefficient and n is the order of the polynomial that can be chosen depending on the energy range of interest. After the relative efficiency calibration curve (11) is constructed, the relative concentrations can be calculated from eq. (3) and converted to absolute concentration using a well-know mass fraction of an element presented in the sample. If the concentration of m elements are required to be analysed there will be $m+n+1$ parameters needed to be optimized in fitting procedure, including a_i, i=0,1,..n and t_k, k=1,2,...m. The iteration loop for determination of all mentioned parameters is presented in Fig. 1.

The loop starts with a reference efficiency curve which is then used for the correction of experimental relative detection efficiency at different energies of all elements, i.e. calculation of all characteristic factors t in eq. 10 (see Fig. 2). In the next step, least-square fitting is performed to construct a new efficiency curve. The Goodness Of Fit (GOF) in the fitting step is used for stop condition. The loop is forced to stop whenever the GOF starts to increase. On the other hand, it will stop if the number of the loop is large enough and the GOF is almost saturated. A typical curve corresponding to the detector used for spectrum acquisition may be chosen as the original reference efficiency curve. It has been found that the employment of different original reference efficiency curves gives a very small divergence on final analysis results.

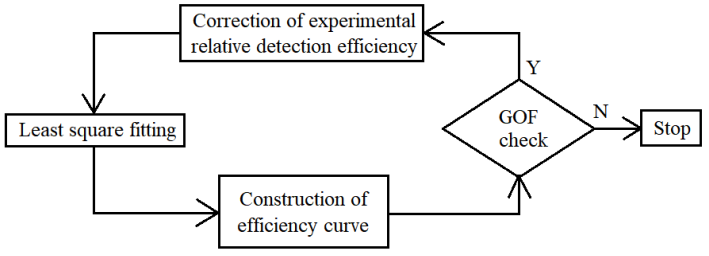

Fig.1. Iteration for optimization of fitting parameters

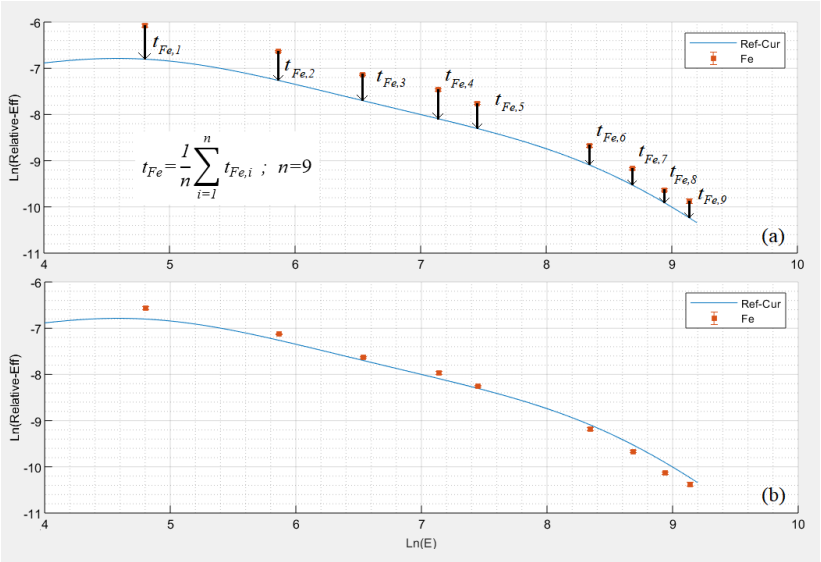

Fig. 2. Illustration of relative efficiency correction for iron by t_{Fe}-factor.
(a) before correction, (b) after correction

For evaluation of the method performance u_{score} test was implemented. u_{score} factor was calculated as follow:

$$u_{score} = \frac{|m_x - m_y|}{\sqrt{\sigma_{m_x}^2 + \sigma_{m_y}^2}} \qquad (12)$$

In this study, the limiting value for u_{score} has been set to 2.58 for a level of probability at 99% to determine if a result passes the evaluation. The u_{score} values less than 1.96 mean that the result probably does not differ significantly from the certified value while u_{score} less than 1.64 that means the result does not differ significantly from the certified value.

B. Results and discussion

In experiments, standard reference materials, BIR-1 and SMELS-III, were used for quality verification of the element concentration for PGNAA and INAA, respectively. BIR-1 sample had been irradiated and analyzed by KFKI lab using k_0 approach. The acquired spectrum was re-used to construct a relative efficiency curve for internal monostandard analysis. In case of INAA, the SMELS III sample was sealed in a polyethylene bag and irradiated for 09 hours at the Rotary Rack channel of Dalat research reactor. The ratio f between thermal and epithermal neutron flux is 37.3 and epithermal neutron spectrum factor α is 0.073 [7]. The measurement was carried out for about ~18 hours after ~5 days of decay. To assess the feasibility of the method, analysis of large samples has been attempted. Two NIST-679 samples of different sizes and weights were prepared and irradiated. The small one (103.25mg) was analyzed by k_0 approach while the large (1.365g) were studied by IM-method using both optimized and non-optimized efficiency curves. Gamma spectrum was acquired by an HPGe detector. The detector solution is 1.90 keV for 1332.5 keV (^{60}Co).

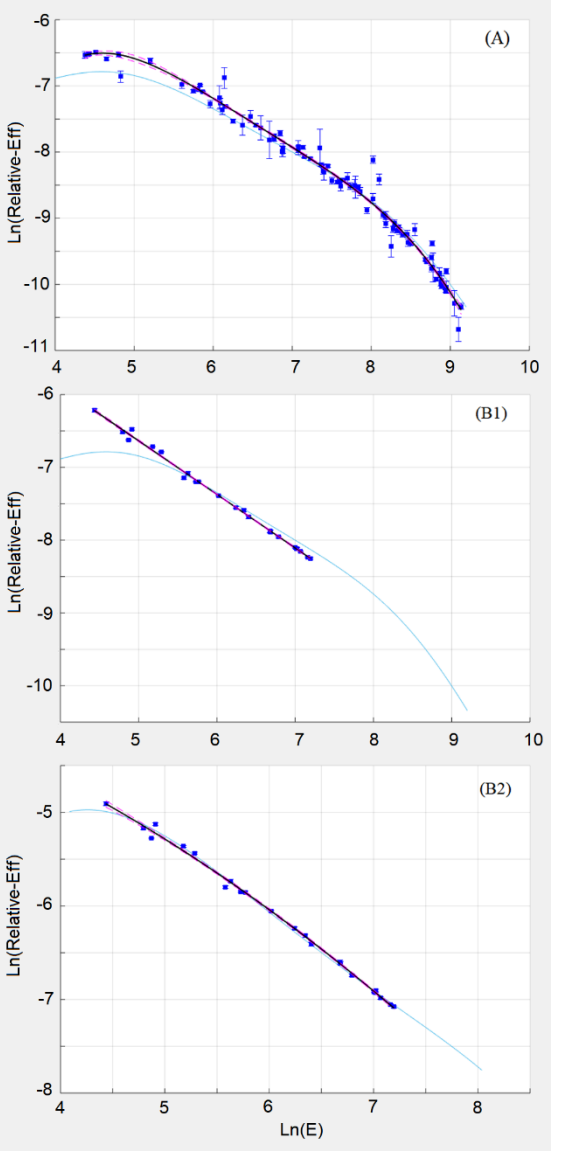

Fig. 3. Construction of in situ relative efficiencies.
(A) BIR-1 sample, original curve 1,
(B1) SMELS-III sample, original curve 1,
(B2) SMELS-III sample, original curve 2.

In situ relative efficiency for each sample has been constructed using the mentioned fitting procedure. Fig. 3 indicates the improvement of efficiency curves before and after fitting steps. As for the BIR-1 sample, the efficiency curve demonstrates a small change at high energy region while in the low energy region the divergence becomes large. To assess the feasibility of the procedure,

two different original efficiency curves were used in the study of the SMELS-III sample. As clearly seen, the obtained relative efficiency curves are very similar, showing the differ from each other by nearly a constant factor of about 1.3 in the logarithm of relative efficiency.

Analysis of element concentration in the samples has been implemented using the orresponding efficiency curve. Table I shows the mass fraction of 15 elements in the BIR-1 sample. A majority of IM's element sconcentration has been found in good agreement with certified values, excluding results for Cr, Mn and Co. However, k_0 approach shows a very similar pattern in case of Cr and Co when the results are about 2 times greater than the certified values.

The situation becomes better when using IM's method in the INAA study of the SMELS-III sample (see Table. II). Despite using different original efficiency curves, the results are convergent and very close to assigned values.

Table I. Concentration found in BIR-1 sample (unit: Oxide form – wt%, Element – ppm)

No.	El	Certified values		k_0-approach (KFKI)		IM-approach			Note
		Conc. (1)	+/- (2)	Conc.	Rel. Unc. (3)	Conc.	+/-	u-score	
1	Na	1.82	0.045	1.82	1.9	1.82	0.06	0.00	Oxide form
2	Mg	9.7	0.079	10	5.	9.4	0.6	0.50	Oxide form
3	**Al***	**15.5**	**0.15**	**15.0**	**2.6**	**15.5**	**0.9**	**0.00**	Oxide form
4	Si	47.96	0.19	48	1.4	45.37	1.47	1.75	Oxide form
5	Ca	13.3	0.12	12.8	3.0	12.5	0.4	1.92	Oxide form
6	Sc	44	1	56	2.7	49.7	3.4	1.61	Element
7	Ti	0.96	0.01	1.01	2.6	0.98	0.03	0.63	Oxide form
8	V	310	11	401	3.5	336	40	0.63	Element
9	Cr	370	8	516	5.	626	47	5.37	Element
10	Mn	0.175	0.003	0.175	2.4	0.203	0.010	2.68	Oxide form
11	Fe	11.3	0.12	11.2	2.4	11.5	0.4	0.48	Oxide form
12	Co	52	2	104	4.0	116	8	7.76	Element
13	Ni	170	6	180	7.	200	37	0.80	Element
14	Sm	1.1	-	0.80	3.6	0.78	0.04	-	Element
15	Gd	1.8	0.4	1.6	5.	1.82	0.11	0.05	Element

Table II. Concentration found in SMELS III sample (unit: ppm)

No.	El.	Assigned values		k_0-approach		IM-approach, original curve 2			IM-approach, original curve 1		
		Conc.	+/-	Conc.	+/-	Conc.	+/-	u-score	Conc.	+/-	u-score
1	Sc	1.140	0.031	1.21	0.01	1.136	0.039	0.08	1.15	0.039	0.2
2	Cr	86.7	2.6	90.01	3.79	83.5	2.9	0.82	88.8	3	0.53
3	**Fe***	**8200**	**190**	**8655**	**357**	**8200**	**190**	**-**	**8200**	**190**	**-**
4	Co	24.3	0.33	25.45	1.04	23.9	0.8	0.46	23.9	0.8	0.46
5	Zn	618	11	660	27	608	21	0.42	610	21	0.34
6	Se	131	6	144	6	133.5	4.9	0.32	143	5	1.54
7	Sr	8150	200	8891	374	7767	272	1.13	8132	286	0.05
8	Cs	20.80	0.34	22.53	0.92	19.5	0.7	1.67	20.1	0.8	0.81
9	Tm	23.3	0.7	25	1	24.6	1.2	0.94	26.2	1.3	1.96
10	Yb	20.7	0.5	22.5	0.9	22.5	0.8	1.91	24.1	0.8	3.6
11	Au	0.901	0.016	-	-	0.832	0.028	2.14	0.879	0.03	0.65

Table III. Concentration found in NIST-679 samples (unit: Fe-wt%, others-ppm)

No.	El.	Datasheet Value's		k_0-approach, Small sample		IM approach Non-optimized efficiency, Large sample		IM-approach Optimized efficiency, Large sample		u-score
		Conc.	+/-	Conc.	+/-	Conc.	+/-	Conc.	+/-	
1	Sc	22.5	-	22.4	0.5	23.3	0.6	23.4	0.7	-
2	Cr	109.7	4.9	120.2	5.5	107.5	2.7	106.7	3.3	0.51
3	**Fe***	**9.05**	**0.21**	**8.95**	**2.2**	**9.05**	**0.21**	**9.05**	**0.21**	-
4	Co	26	-	24.9	0.8	26.3	0.6	26.1	0.7	-
5	Zn	150	-	163	15	130.4	3.5	130.4	3.8	-
6	Rb	190	-	201	17	211.7	6.1	211.8	6.6	-
7	Cs	9.6	-	9.4	0.5	9.6	0.3	9.54	0.36	-
8	Ce	105	-	118	4	98.1	2.6	105.4	3.7	-
9	Eu	1.9	-	1.6	0.1	1.62	0.04	1.65	0.06	-
10	Hf	4.6	-	4.3	0.2	4.54	0.13	4.53	0.16	-

(1) Concentration, (2) Absolute Uncertainty, (3) Relative Uncertainty (%).

*Reference Element

The study of samples of different sizes and weights has been attempted. Table III compares mass fractions of 10 elements presented in NIST-679 samples with certified and informative values. As clearly seen, the difference in sample size and weight gives rise to some variation in obtained relative concentrations of Cr, Zn, Rb, Ce to Fe. If the optimized efficiency curve is employed it can help to correct the results for Ce. However, the difference in sample size and weight gives an insignificant change in the relative efficiency curve. Therefore, it is desired for further verification of the method using large samples of various shape and size.

III. CONCLUSIONS

A procedure for the determination of in situ relative detection efficiencies for internal monostandard neutron activation analysis has been proposed. The element concentration found in some standard samples were in good agreement with certified values. The method is promising as it has been successfully applied to a nonstandard geometrical sample. However, further analysis of large samples of various geometry is required to verify and optimize the method.

ACKNOWLEDGMENT

The authors are thankful to the Ministry of Science and Technology of Vietnamese government for financial support through the ministerial-level project DTCB-01/18-VNCHN.

REFERENCES

[1]. Nguyen Canh Hai, Nguyen Nhi Dien, Vuong Huu Tan, Tran Tuan Anh, Pham Ngoc Son, Ho Huu Thang, "Determination of elemental concentrations in biological and geological samples using PGNAA facility at the Dalat research reactor", *J Radioanal Nucl Chem*, 319 (3), 1165-1171, 2019.

[2]. Rahat Khan, Shayantani Ghosal, Debashish Sengupta, Umma Tamim, Syed Mohammod Hossain, Sudha Agrahari, "Studies on heavy mineral placers from eastern coast of Odisha, India by instrumental neutron activation analysis", *J Radioanal Nucl Chem*, 319 (1), 471-484, 2018.

[3]. Jan Kamenik, Filipa R. F. Simoes, Pedro M. F. J. Costa, Jan Kucera, Vladimir Havranek, "INAA and ion-beam analysis of elemental

admixtures in carbon-based nanomaterials for battery electrodes", *J Radioanal Nucl Chem*, 318 (3), 2463-2472, 2018.

[4]. Pasquale Avino, Geraldo Capannesi, Luigina Renzi, Alberto Rosada, "Physiological parameters affecting the hair element content of young Italian population", *J Radioanal Nucl Chem*, 306 (3), 737-743, 2015.

[5]. Sudarshan, K.; Nair, A. G. C.; Goswami, A. J. Radioanal. "A proposed k0 based methodology for neutron activation analysis of samples of non-standard geometry", *J Radioanal Nucl Chem*, 256 (1), 93-98, 2003.

[6]. A. G. C. Nair, R. Acharya, K. Sudarshan, S. Gangotra, A. V. R. Reddy, S. B. Manohar and A. Goswami. "Development of an internal monostandard instrumental neutron activation analysis method based on in situ detection efficiency for analysis of large and nonstandard geometry samples", *Anal. Chem.* 75, 4868-4874, 2003.

[7]. Manh-Dung Ho, Quang-Thien Tran, Van-Doanh Ho, Dong-Vu Cao, Thi-Sy Nguyen, "Quality evaluation of the k_0-standardized neutron activation analysis at the Dalat research reactor", *J Radioanal Nucl Chem*, 309 (1), 135-143, 2016.